Mon. Not. R. Astron. Soc. **386,** 2253–2261 (2008) doi:10.1111/j.1365-2966.2008.13233.x

Multiwavelength study of the transient X-ray binary IGR J01583+6713

Ramanpreet Kaur,[1★] Biswajit Paul,[2] Brijesh Kumar[1,3] and Ram Sagar[1]

[1] *Aryabhatta Research Institute of Observational Sciences (ARIES), Manora Peak, Nainital 263 129, India*
[2] *Raman Research Institute, C V Raman Avenue, Sadashivanagar, Bangalore 560 080, India*
[3] *Departamento de Física, Universidad de Concepción, Casilla 160-C, Concepción, Chile*

Accepted 2008 March 6. Received 2008 March 6; in original form 2007 December 15

ABSTRACT

We have investigated multiband optical photometric variability and stability of the Hα line profile of the transient X-ray binary IGR J01583+6713. We set an upper limit of 0.05 mag on photometric variations in the V band over a time-scale of three months. The Hα line is found to consist of non-Gaussian profile and quite stable for a duration of two months. We have identified the spectral type of the companion star to be B2 IVe while the distance to the source is estimated to be $\sim$4.0 kpc. Along with the optical observations, we have also carried out analysis of X-ray data from three short observations of the source, two with the *Swift*–XRT and one with the *RXTE*–PCA. We have detected a variation in the absorption column density, from a value of 22.0×10^{22} cm^{-2} immediately after the outburst down to 2.6×10^{22} cm^{-2} four months afterwards. In the quiescent state, the X-ray absorption is consistent with the optical reddening measurement of $E(B - V) = 1.46$ mag. From one of the *Swift* observations, during which the X-ray intensity was higher, we have a possible pulse detection with a period of 469.2 s. For a Be X-ray binary, this indicates an orbital period in the range of 216–561 d for this binary system.

Key words: binaries: general – stars: emission-line, Be – stars: individual: IGR J01583+6713 – pulsars: general – X-rays: stars.

1 INTRODUCTION

The ESA X-ray and γ-ray observatory *INTEGRAL* has discovered more than 100 sources during its continuous monitoring of the sky, especially in the direction of the Galactic Centre and its surroundings, since its launch in 2002. Many of the X-ray sources discovered by *INTEGRAL* are characterized by a hard X-ray spectrum, with little or no detectable emission in soft X-rays, since they are heavily absorbed by interposing material. X-ray characteristics of most of these sources indicate them to be high-mass X-ray binaries and in many cases this has been proved by the discovery of their optical counterparts (e.g. Masetti et al. 2006a; Negueruela et al. 2007).

The X-ray transient IGR J01583+6713 was discovered by the IBIS/ISGRI imager onboard *INTEGRAL* during an observation of the Cas A region on 2005 December 6 (Steiner et al. 2005). The source was detected with a mean flux of about 14 mCrab in the 20–40 keV band, while a null detection was reported in the higher energy band of 40–80 keV. In subsequent *INTEGRAL* observations of the same field during 2005 December 8–10, the X-ray flux was found to be decreasing on a time-scale of days. *Swift* observations of the source on 2005 December 13 identified IGR J01583+6713 to be a point object located at RA: $01^{\rm h}58^{\rm m}18\overset{\rm s}{.}2$ and Dec.: $+67^{\circ}13'25\overset{''}{.}9$ (J2000) with an uncertainty of 3.5 arcsec and its spectral analysis revealed that it is highly absorbed with $N_{\rm H}$ approximately 10^{23} cm^{-2} as compared to the estimated galactic value of $N_{\rm H} = 4.7 \times 10^{21}$ cm^{-2} towards the same direction (Kennea et al. 2005). Follow-up optical and infrared (IR) observations identified the X-ray source as a Be star with magnitudes – $B = 14.98$, $R = 13.24$ and $I = 12.12$, displaying strong Hα [equivalent width (EW) = 70 Å] and weak Hβ (EW = 6 Å) lines in emission and it was therefore proposed as the optical/IR counterpart of the X-ray source (Halpern et al. 2005). Recently, based on low-resolution single-epoch optical spectroscopy on 2006 December 23, Masetti et al. (2006b) classified the counterpart as an early spectral type (O8 III or O9 V) Galactic ($\sim$6.4 kpc) star and ruled out the possibility of both a supergiant companion and the source being a low-mass X-ray binary or a cataclysmic variable.

In this paper, we present results of new optical (photometric and spectroscopic) observation of the Be system over an extended period and analyse all the X-ray data on IGR J01583+6713 present in the HEASARC archive. Sections 2 and 3 present the observations and data reduction. Section 4 deals with the results and discussions on the nature of the companion star, possible variability and characterization of the X-ray spectrum. We summarize the results in the last section.

★E-mail: raman@aries.ernet.in

Table 1. Log of broad-band optical photometric observations of the transient source and Landolt (1992) standard fields.

Object	Date of observation	Filter	Exposure time (s)
IGR J01583+6713			
	2005 December 13	*V*/*R*	2 × 600/2 × 300
	2005 December 17	*B*/*V*/*R*/*I*	2 × 300/2 × 300/3 × 200/2 × 150
	2005 December 18	*B*/*V*/*R*/*I*	3 × 300/3 × 300/3 × 150/3 × 150
	2005 December 19	*V*/*R*/*I*	1 × 300/1 × 200/1 × 150
	2005 December 20	*B*/*V*/*R*/*I*	1 × 300/2 × 300/1 × 300/3 × 150
	2005 December 21	*R*/*I*	1 × 150/2 × 150
	2005 December 28	*B*/*V*/*R*/*I*	1 × 300/2 × 300/2 × 200/3 × 150
	2006 January 25	*B*/*R*/*I*	1 × 300/2 × 200/1 × 150
	2006 January 26	*B*/*V*/*R*/*I*	1 × 300/2 × 300/2 × 200/2 × 150
	2006 February 24	*B*/*V*/*R*	2 × 300/2 × 300/2 × 200
	2006 February 28	*V*/*R*	1 × 300/1 × 200
	2006 March 2	*U*/*B*/*V*/*R*/*I*	2 × 300/2 × 300/2 × 300/2 × 200/2 × 150
	2006 March 6	*B*/*V*/*R*	1 × 300/1 × 300/1 × 200
	2006 November 24	*U*/*B*/*V*/*R*/*I*	2 × 300/2 × 300/2 × 300/2 × 200/2 × 150
	2006 December 13	*U*/*B*/*V*/*R*/*I*	3 × 300/3 × 300/3 × 300/2 × 200/2 × 150
Landolt standard field			
SA104	2006 January 25	*B*/*R*/*I*	11 × 300/11 × 60/11 × 60
SA101	2006 March 2	*U*/*B*/*V*/*R*/*I*	9 × 300/9 × 180/9 × 180/9 × 120/9 × 120
SA92	2006 November 24	*U*/*B*/*V*/*R*/*I*	2 × 300/2 × 300/2 × 180/2 × 130/2 × 100
SA95	2006 November 24	*U*/*B*/*V*/*R*/*I*	7 × 500/7 × 300/7 × 150/7 × 100/7 × 100
SA98	2006 December 13	*U*/*B*/*V*/*R*/*I*	7 × 450/7 × 300/7 × 120/7 × 60/7 × 60
RU149	2006 December 13	*U*/*B*/*V*/*R*/*I*	2 × 300/2 × 300/2 × 120/2 × 60/2 × 60

2 OPTICAL OBSERVATIONS

The broad-band photometric and intermediate-resolution spectroscopic optical observations are described in the following sections.

2.1 *UBVRI* photometry

We have carried out broad-band Johnson *UBV* and Cousins *RI* CCD photometric follow-up observations on 13 nights from 2005 December 13 to 2006 March 6 using a 2k × 2k CCD camera mounted at f/13 Cassegrain focus of the 104-cm Sampurnanand Telescope (ST) at ARIES, Nainital, India. At the focus, a 24 μm square pixel of the 2048 × 2048 size CCD chip corresponds to ∼0.36 arcsec and the entire chip covers a square area of side ∼13.0 arcmin on the sky. The read-out noise of the system is 5.3 electrons with a gain factor of 10 electrons per analog-to-digital unit. During our observations the seeing varied from about 1.2 to 2.4 arcsec. Table 1 lists the log of optical photometric observations of IGR J01583+6713 in *UBVRI* wavebands along with the number of frames taken and exposure time in the respective filters. Usually more than two exposures were taken in each filter with typical exposure times of 300, 300, 300, 200 and 150 s in the *U*, *B*, *V*, *R* and *I* wavebands, respectively. Bias frames were taken intermittently and flat-field exposures were made of the twilight sky. In addition, as part of other ongoing programmes, we could secure observations of Landolt (1992) standard fields in *UBVRI* wavebands on four nights (see Table 1) near zenith and the same field was also observed at about five different zenith distances for extinction measurements.

Fig. 1 shows the field chart of IGR J01583+6713 observed with ST on 2006 December 13 in the *B* waveband. Although all the observations were taken with the entire CCD chip of 13 × 13 arcmin^2, we have shown only a 7.5 × 7.5-arcmin^2 CCD frame in Fig. 1 for a closer look at the field. For a photometric comparison, we selected six stars with similar brightness and these are marked as 1, 2, 3, 4, 5 and 6 in Fig. 1 while 'T' denotes the X-ray transient IGR J01583+6713.

Photometric data reductions were performed using the standard routines in IRAF[1] and DAOPHOT (Stetson 1987). The zero-points and colour terms were applied in the usual manner (Stetson 1992). The standard magnitudes of all six stars were found to be stable on all four nights and were treated as local standards. Their mean standard magnitudes are listed in Table 2. The mean magnitudes and colours for IGR J01583+6713 are estimated as $V = 14.43 \pm 0.03$, $U - B = 0.09 \pm 0.04$, $B - V = 1.22 \pm 0.07$, $V - R = 0.99 \pm 0.03$ and $V - I = 1.88 \pm 0.05$. The differences in the measured ($B_{\rm obs}$, $V_{\rm obs}$, $R_{\rm obs}$ and $I_{\rm obs}$) and standard ($B_{\rm st}$, $V_{\rm st}$, $R_{\rm st}$ and $I_{\rm st}$) *BVRI* magnitudes of IGR J01583+6713 and comparison star 1 are plotted in Fig. 2. The variation was observed to be consistent with the typical photometric uncertainty with standard deviations of 0.01 mag for *BVR* and 0.02 mag for the *I* passband for comparison star 1. For IGR J01583+6713, an increase in flux of about 0.05 mag is apparent around 2005 December 13, followed by a constant flux level thereafter.

2.2 Spectroscopy

Spectroscopic observations of IGR J01583+6713 were made on eight nights during 2006 August 18 to 2006 October 28 using the Himalayan Faint Object Spectrograph and Camera (HFOSC) available with the 2-m Himalayan Chandra Telescope (HCT), located at Hanle, India. The pixel size of the CCD used is 15 μm with an image scale of 0.297 arcsec pixel^{-1}. The log of observations with the respective exposure times is given in Table 3. We have used a slit of dimensions 1.92 arcsec × 11 arcmin for the Hα line profile study and a slit of dimensions 15.41 arcsec × 11 arcmin for the

[1] IRAF is distributed by the National Optical Astronomy Observatories, USA.

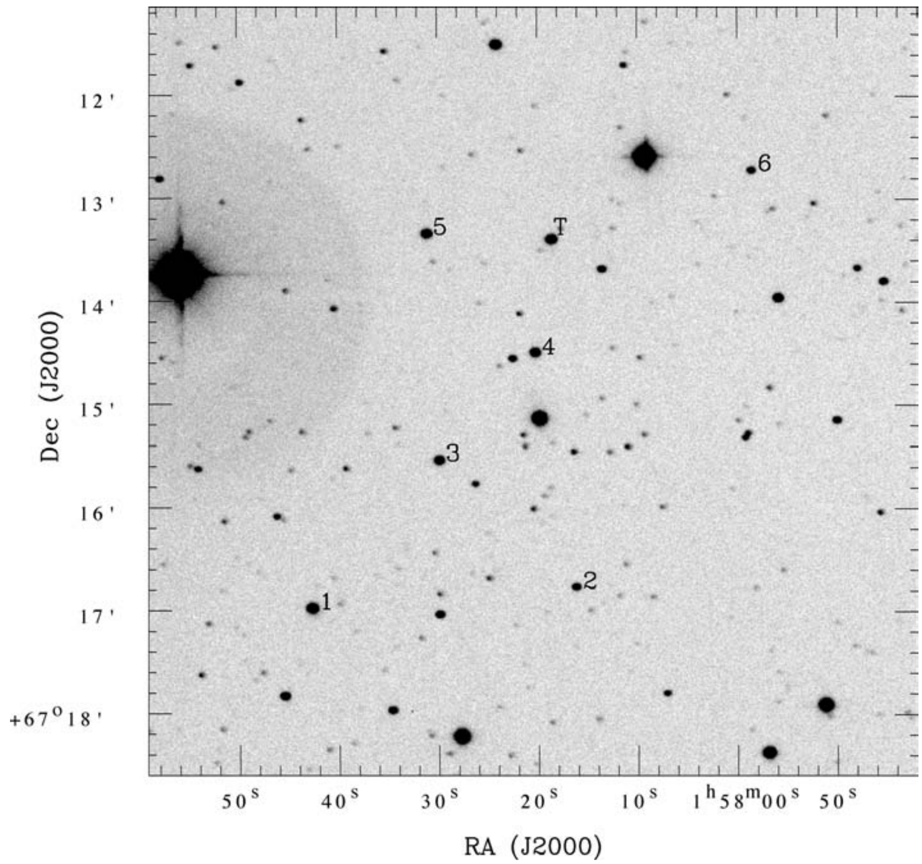

Figure 1. Identification chart of IGR J01583+6713 taken with ST in *B* passband on 2006 December 13. The transient is marked as 'T' and comparison stars are marked as 1, 2, 3, 4, 5 and 6 in the figure.

Table 2. *BVRI* magnitudes of comparison stars.

Star number	*B*	*V*	*R*	*I*
1	15.55	14.51	13.91	13.37
2	17.57	15.45	14.17	13.00
3	16.54	15.38	14.68	14.02
4	16.25	14.92	14.11	13.36
5	16.13	14.73	13.90	13.20
6	17.71	15.52	14.20	12.99

calibration observations. The spectra were obtained with two different gratings (Grism 7 and Grism 8) in the wavelength range of 3500–7000 and 5800–8350 Å at a spectral dispersion of 1.45 and 1.25 Å pixel^{-1}, respectively. Data were reduced using the standard routines within IRAF. The data were bias-corrected, flat-fielded and the one-dimensional spectrum extracted using the optimal extraction method (Horne 1986). The wavelength calibration was done using FeAr and FeNe lamp spectrum for the Grism 7 and Grism 8 spectrum, respectively. We employed the IRAF task IDENTIFY and typically around 18 emission lines of Fe, Ar and Ne were used to find a dispersion solution. A fifth-order fit was used to achieve a typical rms uncertainty of about 0.1 Å. For flux calibration of the IGR J01583+6713 spectrum in both Grism 7 and Grism 8, the instrumental response curves were obtained using spectrophotometric standards (Hiltner 600, Feige 110) observed on the same night, and the star's spectra were brought to the relative flux scale. Hα is detected with a full width at half-maximum of ∼11.3 Å for all the spectra taken with Grism 8 of HCT.

The combined flux-calibrated spectrum of the X-ray binary IGR J01583+6713, taken with Grism 7 and Grism 8 on 2006 October 15, is shown in Fig. 3 over a wavelength range of 3800–9000 Å. The identified spectral features are marked in the spectrum. The blue region of Grism 7, in the wavelength region 3600–3800 Å, has a poor signal-to-noise ratio and is not shown in Fig. 3. Along with strong Hα and Hβ, we also detected a few weak spectral features, mainly singly ionized iron, neutral helium and neutral oxygen lines, in the IGR J01583+6713 continuum spectrum in the wavelength region 6100–7900 Å, shown in Fig. 4.

3 X-RAY OBSERVATIONS

The X-ray observations of IGR J01583+6713 were carried out with the X-ray Telescope (XRT) onboard the *Swift* satellite and with the Proportional Counter Array (PCA) onboard the *RXTE* satellite.

Swift carried out observations of IGR J01583+6713 on 2005 December 13 for 47 ks and on 2006 April 11 for 37 ks. Both the XRT observations had useful exposures of ∼8 ks. The standard data pipeline package (XRTPIPELINE v0.10.3) was used to produce screened event files. Only data acquired in the photon counting (PC) mode were analysed adopting the standard grade filtering (0–12 for PC) according to XRT nomenclature. X-ray events from within a circular region of radius 0.8 arcmin, centred at the X-ray transient, were extracted for timing and spectral analysis. Background data were extracted from a neighbouring source-free circular region of

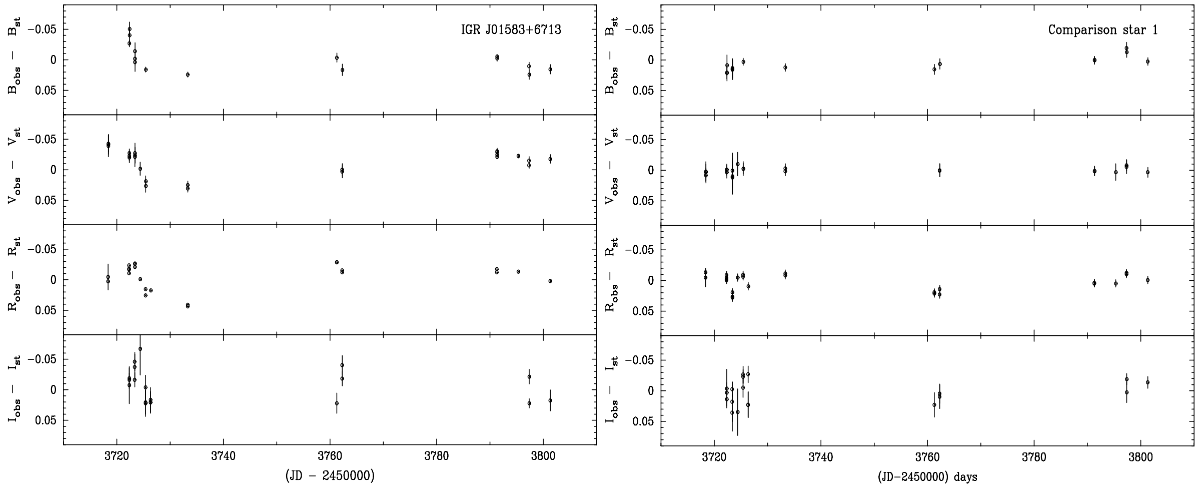

Figure 2. The difference in the measured (B_{obs}, V_{obs}, R_{obs} and I_{obs}) and standard (B_{st}, V_{st}, R_{st} and I_{st}) *BVRI* magnitudes of IGR J01583+6713 and comparison star 1 from JD 245 3710 to JD 245 3810.

Table 3. Log of spectroscopic observations of the X-ray transient IGR J01583+6713.

Date of observation	Wavelength range (Å)	Exposure time (s)
2006 August 18	3500–7000:5200–9200	1 × 900/1 × 900
2006 October 14	3500–7000:5200–9200	1 × 900/1 × 900
2006 October 15	3500–7000:5200–9200	1 × 1200/1 × 900
2006 October 16	5200–9200	1 × 900
2006 October 17	5200–9200	1 × 900
2006 October 18	3500–7000:5200–9200	1 × 900/1 × 900
2006 October 28	5200–9200	1 × 900
2006 October 29	5200–9200	1 × 600

the same radius as taken for the source. Source and background light curves were generated using the X-ray counts from the respective circular regions with the instrumental time-resolution of 2.5074 s. A final source light curve was produced by subtracting the background light curve. The observations were made for small segments and no variability beyond statistical variation is seen in the X-ray light curves between the segments. The final source spectrum were obtained by subtracting the background spectrum, and spectral analysis was done using the energy response of the detector for the same day.

RXTE pointed observations were performed on 2005 December 14 with a total effective exposure time of ∼3 ks. The *RXTE*-PCA standard 2 data with a time-resolution of 16 s were used to extract

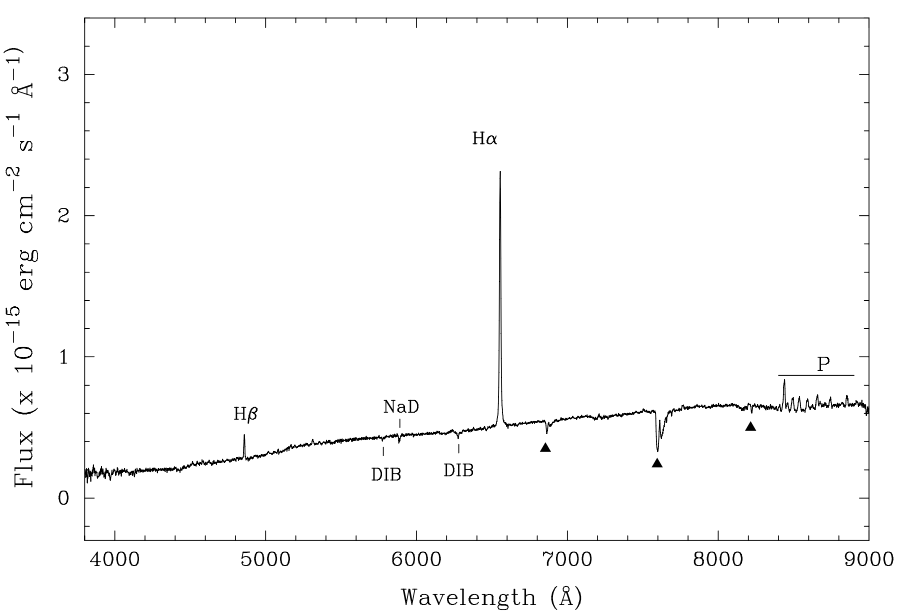

Figure 3. Flux-calibrated spectrum of IGR J01583+6713 taken on 2006 October 15. Grism 7 and Grism 8 spectra are combined together to show it over a wavelength range of 3800–9000 Å. Diffuse interstellar bands are marked as ‘DIB’, telluric absorption bands are marked with a filled triangle and the sodium doublet is marked as ‘NaD’. ‘P’ represents Paschen lines. Hα and Hβ are also marked.

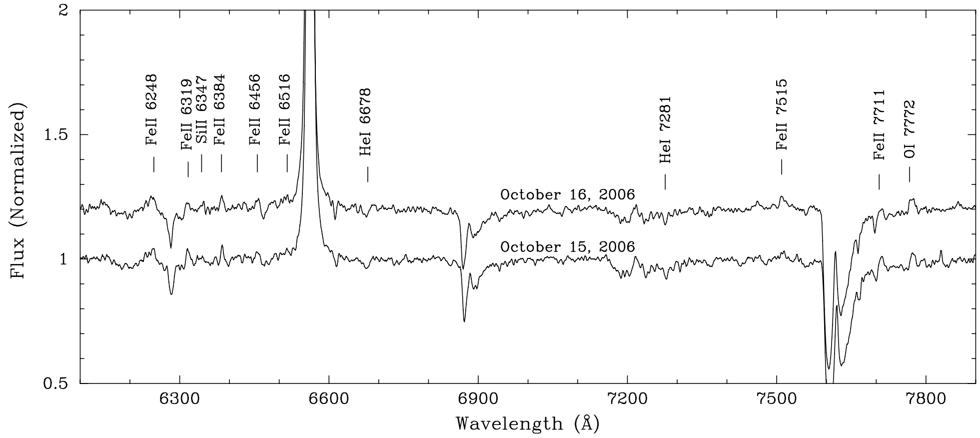

Figure 4. Continuum spectrum of IGR J01583+6713 in the wavelength range of 6100–7900 Å taken on 2006 October 15 and October 16. A few weakly identified features like Fe II, He I, Si II and O I are marked in the figure.

the spectrum of the source in the energy range 3–20 keV. During this observation only two PCUs were operational. The background spectrum for this observation was generated using the task 'PCABACKEST'. PCA background models for faint sources were used to generate the background spectrum. The spectral response matrix of the detector was created using the task 'PCARSP' and applied for spectral fitting. The spectrum was rebinned to have a sufficient signal-to-noise ratio in each bin of the spectrum. The source was also regularly monitored by the All Sky Monitor (ASM) onboard *RXTE*. The ASM light curve is shown in Fig. 5 from MJD 536 60 to MJD 541 60, including the outburst detected on MJD 537 10. The epoch of detection of the hard X-ray transient IGR J01583+6713 is marked as 'T' in Fig. 5. The soft X-ray enhancement in the *RXTE*-ASM light curve is consistent with a 10–20 mCrab intensity. The optical and X-ray observations of IGR J01583+6713 taken for this study are also marked in Fig. 5.

We have used XSPEC12 for X-ray spectral analysis. We fitted both a power-law model and a blackbody model with line-of-sight absorption to the source spectrum obtained from *Swift* and *RXTE*. The spectral parameters obtained for both the models for the three observations are given in Table 4. Both the power-law and blackbody models fit the data well with a reduced χ^2 in the range of 0.8–1.4, except for the *RXTE* spectrum which is not well fitted by a blackbody model. Models are indistinguishable from spectral fit only. Fig. 6 shows the power-law fit to the *Swift* observations made on 2005 December 13 (top panel), *RXTE* observations made on 2005 December 14 (middle panel), and *Swift* data taken on 2006 April 5 (bottom panel).

The *Swift* spectra for both the observations made on 2005 December 13 and 2006 April 5 have coarse energy binning, making the iron emission line at 6.4 keV undetectable in the raw spectrum.

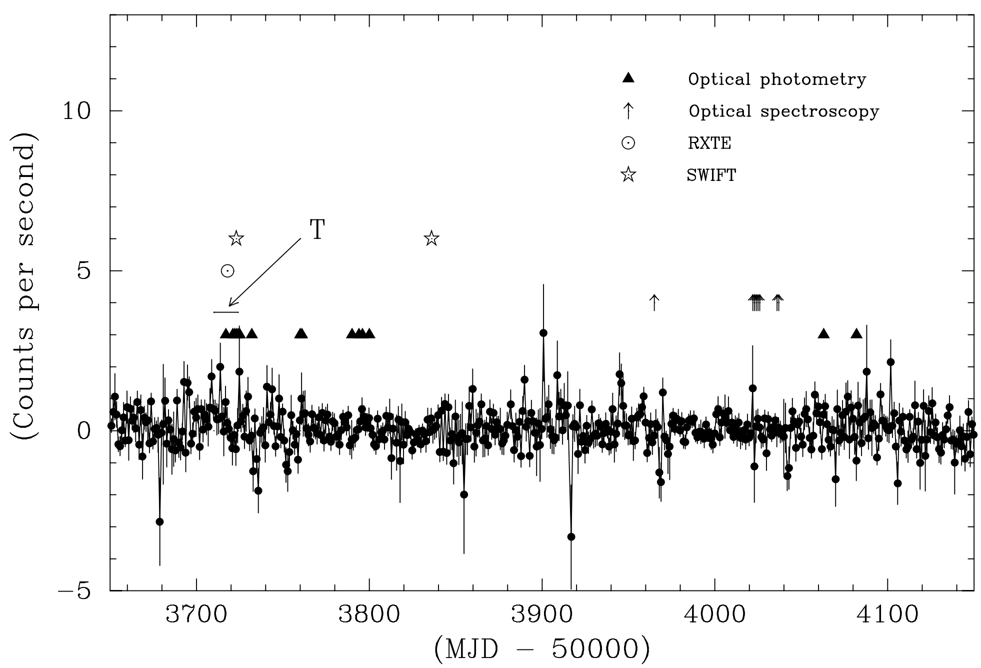

Figure 5. ASM light curve of IGR J01583+6713 from MJD 536 60 to MJD 541 60 including the outburst observed by *INTEGRAL* and *Swift* during MJD 537 10 to MJD 537 20, marked as 'T' in the figure. Also marked are optical photometric observations (by a filled triangle), optical spectroscopic observations (by an up-arrow), *RXTE* observations (by the open circles with a dot inside) and *Swift* observations (by an open star).

Table 4. Spectral parameters for *Swift* and *RXTE* observations.

	RXTE	*Swift*	
	Spectral parameters of a model (absorption + power law)		
Parameter	2005 December 14	2005 December 13	2006 April 05
$N_H \times 10^{22}$ (cm^{-2})	<6.0 (with 90 per cent confidence)	21.96 ± 9.60	2.58 ± 1.06
Photon index	1.71 ± 0.22	1.74 ± 0.56	2.05 ± 0.60
Reduced χ^2/d.o.f.	1.4/14	0.8/19	1.1/13
Observed flux 2–10 keV (erg cm^{-2} s^{-1})	5.0e−12	11.6e−12	3.1e−12
Unabsorbed flux 2–10 keV (erg cm^{-2} s^{-1})	5.5e−12	29.7e−12	4.0e−12
	Spectral parameters of a model (absorption + blackbody)		
Parameter	2005 December 14	2005 December 13	2006 April 5
$N_H \times 10^{22}$ (cm^{-2})	<1.5 (with 90 per cent confidence)	15.16 ± 6.23	0.45 ± 0.22
Blackbody temperature (keV)	1.61 ± 0.44	1.81 ± 0.49	1.34 ± 0.10
Reduced χ^2/d.o.f.	2.5/14	0.8/19	1.2/13
Observed flux 2–10 keV (erg cm^{-2} s^{-1})	5.1e−12	10.8e−12	3.7e−12
Unabsorbed flux 2–10 keV (erg cm^{-2} s^{-1})	5.8e−12	19.6e−12	3.9e−12

To find the upper limit on the 6.4 keV emission line in the *Swift* spectrum taken on 2005 December 13, we fixed the line-centre energy at 6.4 keV in the spectrum and fitted a Gaussian to the line. The upper limit on the EW of the 6.4-keV emission line is determined to be 100 eV with 90 per cent confidence limit.

We searched for X-ray pulse periods using a pulse-folding technique. The background count rate was subtracted from the IGR J01583+6713 light curve and the barycentre correction was done. The time-resolution of the instrument and the time-span of the continuous data constrained the pulse period search to the range 5–800 s. We found X-ray pulsations with a pulse period of 469.2 s and with a pulsed fraction of 22 per cent. Fig. 7 shows the light curve of IGR J01583+6713, observed with *Swift* on 2005 December 13, folded with the pulse period of 469.2 s. However, the evidence of pulsation detection is marginal with a false-alarm-probability of 10^{-4}.

4 RESULTS AND DISCUSSIONS

4.1 Photometric variability

There were seven photometric observations made in 15 d from 2005 December 13 to 2005 December 28 and later on there were observations with a gap of 20–25 d for the next three months. No variability of more than 2σ is found in any passband but a larger variation and decreasing trend is seen for the first few days of observations in all of the passbands, as shown in Fig. 2. The scatter in data points of IGR J01583+6713 is more than the comparison stars by $\sim 2\sigma$ in all the passbands and some increase in magnitude of about 0.05 mag can be seen around MJD 537 25. The decrease in reprocessed optical emission for few days of outburst does indicate that source flux was decreasing during that period. However, we claim no strong variability in this source and we cannot ascertain whether the source was brighter in the optical band during the peak of its X-ray outburst.

4.2 Stability of the Hα emission line

The dynamical evolution of Be envelope can be studied with the help of changes in emission-line profile (Negueruela et al. 2001). Table 3 shows the spectroscopic observations of IGR J01583+6713 made over a period of two months. Strong Hα and Hβ emission-line features are always found in the spectrum with EWs of -74.5 ± 1.6 and -5.6 ± 0.3 Å, respectively. This ratio is somewhat different from that reported by Masetti et al. (2006b), which may indicate structural changes in the circumstellar disc of Be star in this system.

The line EW and line profile of the Hα line are found to be constant for the observations, listed in Table 3. The resolution of our instrument was not good enough to carry out a detailed study of the Hα line shape. The Hα line gives a poor fit with a Gaussian model, leaving the wings of the line unfitted. However, the Hα line, being very strong, of EW = −75 Å, confirms that it originated in the circumstellar disc.

4.3 X-ray variability and spectrum

X-ray observations of IGR J01583+6713 were made on 2005 December 13 by *Swift* after the detection of its outburst on 2005 December 6 by *INTEGRAL*. The pulsations at 469.2 s were detected with a pulsed fraction of 22 per cent. Corresponding to 469.2 s pulse period, we have estimated the X-ray binary IGR J01583+6713 orbital period in the range 216–561 d (Corbet 1986) assuming the maximum eccentricity of the orbit to be 0.47 for Be binaries as observed by Bildsten et al. (1997).

Fig. 6 (top and bottom panels) shows the power-law fitting to the *Swift* observations made on 2005 December 13 and 2006 April 5. N_H is found to decrease from 22.0×10^{22} to 2.6×10^{22} cm^{-2} for the two *Swift* observations of IGR J01583+6713, using the power-law model. Using the blackbody model, N_H is found to decrease from 15.2×10^{22} to 0.5×10^{22} cm^{-2}. Photon index and blackbody temperature are in the range 1.7–2.0 and 1.3–1.8 keV, respectively, for all the observations listed in Table 4. *Swift* observations clearly show that N_H has decreased by about an order of magnitude in a span of four months. The observed flux in 2–10 keV band has also decreased by a factor of ∼4. Within measurement uncertainty, the power-law photon index (or the blackbody temperature in the blackbody emission model) is found to be unchanged.

Lack of variability in the optical photometric measurements indicates an absence of changes in the distribution of circumstellar material around the companion star. However, from the X-ray spectral measurements we have detected a significant change in the absorption column density. During the first *Swift* observations, when the source was brighter, we measured an absorption column density of $(22 \pm 10) \times 10^{22}$ cm^{-2} and the spectrum shows an upper

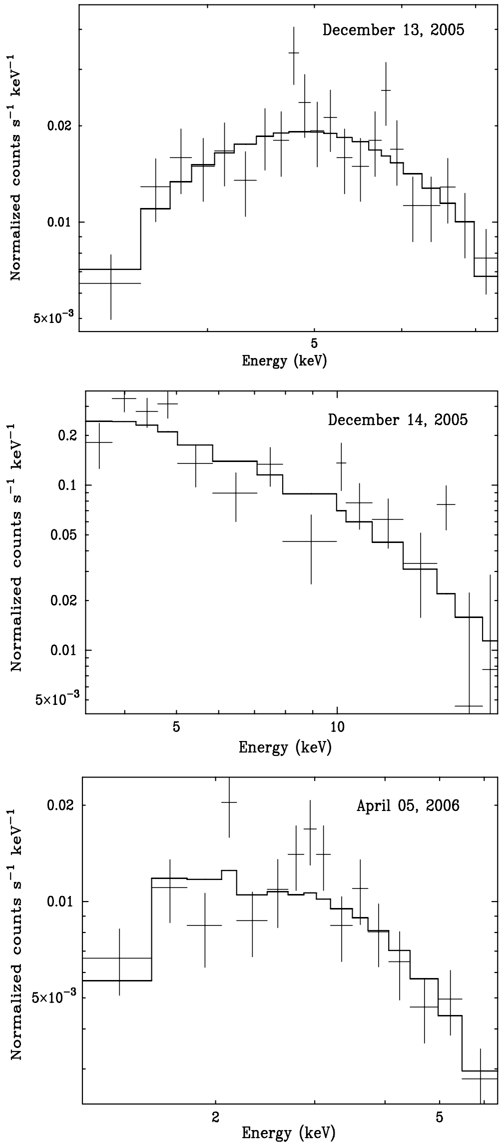

Figure 6. X-ray spectrum of IGR J01583+6713. Top panel: *Swift* observations made on 2005 December 13, middle panel: *RXTE* observations on 2005 December 14, and bottom panel: *Swift* observations made on 2006 April 5. The points with error bars are the measured data points and the histograms are the respective best-fitted model spectrum consisting of absorbed power-law model components, convolved with the respective telescope/detector responses.

limit of 100 eV on the EW of an iron K-fluorescence line. If we assume an isotropic distribution of absorbing matter around the compact object, where the X-ray emission originates, we expect the Fe 6.4 keV spectral line to be detected with an EW of 250 eV (Makishima 1986), a factor of 2.5 more than the upper limit. The absence of a strong iron emission line indicates that the X-ray absorbing material around the compact object has a non-isotropic distribution, probably related to its disc structure.

4.4 Spectral classification

A low-dispersion (4 Å pixel^{-1}) optical (3500–8700 Å) spectrum taken one day after the outburst was presented by Masetti et al.

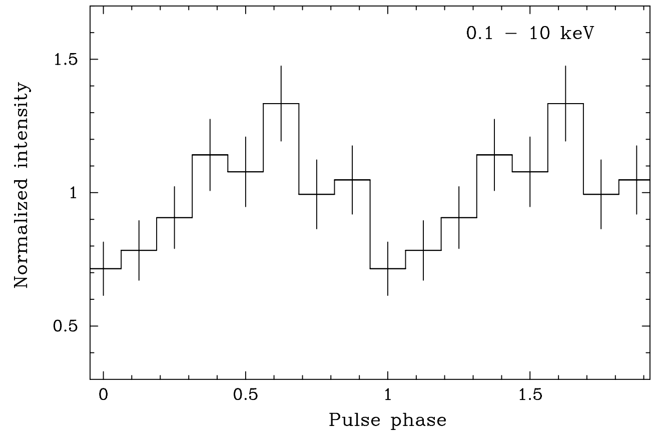

Figure 7. Light curve of IGR J01583+6713 observed by *Swift* on 2005 December 13, folded modulo 469.2 s.

(2006b). However, due to the absence of any photospheric absorption feature and poor signal, they could not secure a definite classification so assuming a Galactic reddening and $(B - R)_0$ intrinsic colour they assigned a spectral type of O8III or O9V. The present spectra cover the same spectral region and have a better spectral resolution (∼3 Å near Hα); however, the MK classical region (<5000 Å) was too weak to identify absorption features. Fig. 3 shows the combined flux calibrated spectrum of IGR J01583+6713 on 2006 October 15. The continuum normalized spectra taken on 2006 October 15 and October 16 are shown in Fig. 4. Most of the spectral features in the 3800–8800 Å region are identified and marked. We compare these features with a near-IR spectral library by Andrillat, Jaschek & Jaschek (1988, 1990) of a sample of 70 emission-line Be stars with known MK spectral type (B0–B9) at resolution (1.2 Å). We describe the spectrum as following.

Hydrogen lines are seen in emission. Hα and Hβ show single peak while the Pashcen lines (P12–P20) have a double-peak structure with the red (R) peak greater than the blue (V) one. Ca II (8498, 8542 and 8662 Å) and N I (multiplet at 8630 and 8680 Å) are also in emission. In their sample, Andrillat et al. (1990) found that the H I and Ca II emission features are strong in early-type (<B5) stars and diminish strongly for later-type stars. Ca II triplet emission was associated with a large *IRAS* excess.

The present spectrum also shows O I (8446 Å and triplet 7773 Å) in emission which is seen in most of the cases with stars having spectral type earlier than B2.5. The features of IGR J1583+6713 resemble most closely HD 164 284 (B2 IV–Ve) in Andrillat et al. (1988) and HD 41335 (B2 IVe) in Andrillat et al. (1990). For a comparison, HD 164284 spectrum is shown on the top of the IGR J01583+6713 spectrum in Fig. 8 over a wavelength range of 7500–8800 Å.

Fe II (6248, 6319, 6384, 6456, 6516, 7515 and 7711 Å) and Si II (6347 Å) lines appear in emission. He I lines at 6678 and 7281 are in absorption with asymmetric profiles indicating the presence of an emission region. Based on these characteristics, it is suggested that its spectral type lies around B1–B3; however, a later spectral type cannot be completely ruled out and a further high-resolution spectrum in the optical and near-IR would be required to ascertain the true spectral type for the transient. Furthermore, the weak Fe 6.4-keV line (EW $\leqslant$ 100 eV) in the X-ray spectrum and a high hydrogen column density may suggest the presence of a wind-powered accretion disc, hence leaving the possibility of a low-luminosity blue supergiant open. However, the strong hydrogen lines suggest that

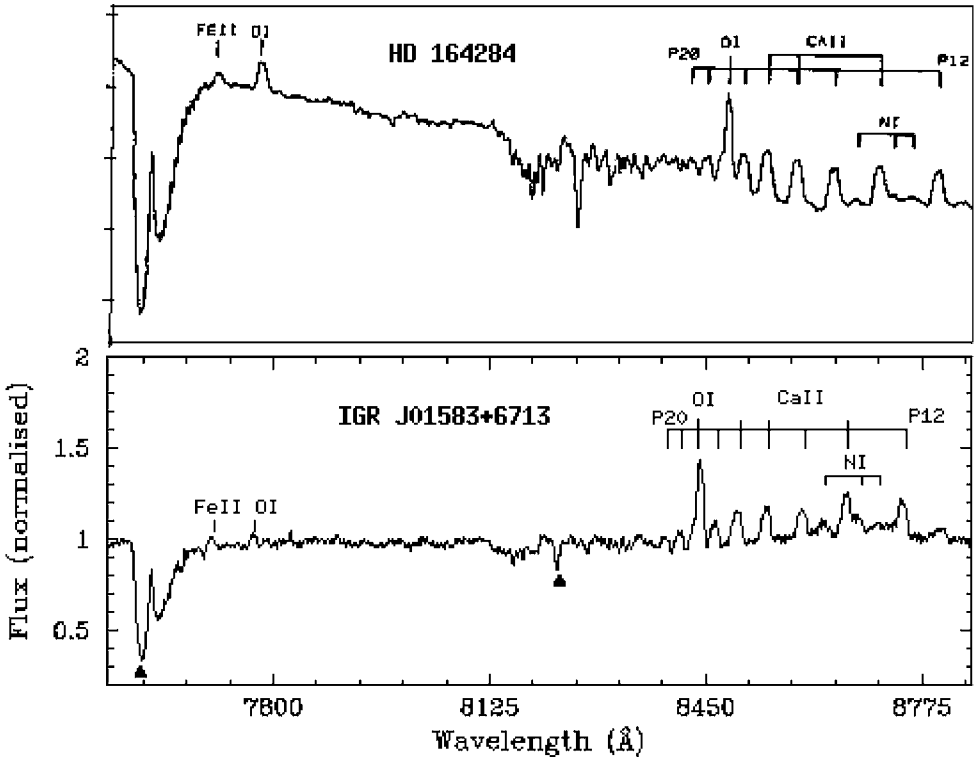

Figure 8. Bottom panel: flux-normalized spectrum of IGR J01583+6713, and top panel: flux-calibrated spectrum of HD 164284 from Andrillat, Jaschek & Jaschek (1988), a comparison. P12–P20 are the hydrogen Paschen lines from P12 to P20. Fe II, O I, Ca II and N I spectral features are also marked in the figure.

it belongs to a main-sequence (IV–V) luminosity class (Leitherer 1988).

We employed the reddening free Q parameter to further ascertain the spectral type of the star. Using the normal reddening slope, $X[E(U-B)/E(B-V)] = 0.72$, the $Q[=(U-B) - X(B-V)]$ parameter was found to be -0.63 ± 0.06 and this corresponds to a spectral type of B2–3 for an early-type main-sequence star (Johnson & Morgan 1954).

We derive a colour excess $E(B-V) = 1.46 \pm 0.05$ mag by adopting B2 IV as a companion and taking the intrinsic colour $(B-V)_0 = -0.24$ mag (Schmidt-Kaler 1982) and a mean observed colour of 1.22 ± 0.05 mag. An estimate of reddening at other wavelengths is made following Fitzpatrick (1999) and the intrinsic colours are found to be $(U-B)_0 = -1.00$, $(V-R)_0 = -0.15$ and $(V-I)_0 = -0.35$ quite consistent with intrinsic colours corresponding to a B2 IV star with $(U-B)_0 = -0.86$ (Schmidt-Kaler 1982), $(V-R)_0 = -0.10$ and $(V-I)_0 = -0.29$ (Wegner 1994). The above colour excesses yield a value of visual extinction $A_V = 4.5 \pm 0.2$ mag. Using the absolute magnitude from Lang (1992), and from the relation $m - M = 5\log D - 5 + A_V$, the distance to the source is estimated to be 4.0 ± 0.4 kpc placing the transient well beyond the Perseus arm of the Milky Way.

For $A_V \sim 4.5$, the corresponding column density N_H is $\sim 8.1 \times 10^{22}$ cm^{-2}. The X-ray observations made by *Swift* during the quiescent state of the transient IGR J01583+6713 on 2006 April 5 gave N_H of the order of 0.5×10^{22} cm^{-2} for blackbody fit and 3×10^{22} cm^{-2} for the power-law fit. The galactic H I column density is 0.4×10^{22} cm^{-2} in the direction of the transient. However, the N_H obtained using the power-law model is closer to the N_H calculated using optical extinction measurement as compared to the blackbody model. Thus, we conclude that the power-law model fits better to the X-ray data than the blackbody spectrum. The power-law index is found to be varying between 1.7 and 2.0, which is common in accretion-powered X-ray pulsars.

5 SUMMARY

The nature of the hard X-ray transient IGR J01583+6713 and its optical counterpart has been investigated using new photometric and spectroscopic data in the optical as well as the X-ray band. Over a one year period since the X-ray outburst (2005 December 6), *UBVRI* CCD photometric data were collected on 15 nights using the 1-m ST optical telescope at Nainital. The intermediate-resolution (3 Å at Hα) spectrum in the 3800–8800 Å region was monitored with the 2-m HCT telescope at Hanle, India, on eight nights. In X-ray, the archival spectral and timing data from *Swift* and *RXTE* observations were analysed to probe the nature of this highly obscured X-ray source. The main conclusions of the study are as follows.

(i) No significant variability in *V* band is seen; however, an upper limit of 0.05 mag is set over a time-scale of three months since the X-ray outburst.

(ii) The spectral characteristics of the optical counterpart were found to be consistent with a B2 IV (classical Be) star showing strong emission lines of hydrogen (single-peak Balmer and double-peak Paschen), ionized calcium, ionized silicon, oxygen, nitrogen and ionized iron. The source is located ($l = 129°, b = 5°$) well beyond the Perseus arm of the Milky Way at a heliocentric distance of $\sim 4.0 \pm 0.4$ kpc.

(iii) We derive a hydrogen column density of 22.0×10^{22} cm^{-2} from the X-ray spectrum taken with *Swift* just after the outburst. The quiescent phase column density was found to be consistent with the optical extinction measurements. The timing measurement suggests a pulse period of 469.2 s and an orbital period in the range of 216–561 d for this binary system.

ACKNOWLEDGMENTS

We thank the referee Juan Fabregat for suggestions that helped us to improve this paper. We thank Dr Maheswar Gopinathan and Mr. Manash Samal for the useful discussions on spectroscopy. One of the authors (Ramanpreet) thanks Jessy Jose and Kuntal Misra for their help with the photometric data reduction and Dr Anna Watts for kindly going through the draft version of this paper. This research has made use of data obtained through the High Energy Astrophysics Science Archive Research Centre Online Service, provided by the NASA/Goddard Space Flight Center.

REFERENCES

Andrillat Y., Jaschek M., Jaschek C., 1988, A&AS, 72, 129
Andrillat A., Jaschek M., Jaschek C., 1990, A&AS, 84, 11 (AND90)
Bildsten L. et al., 1997, ApJS, 113, 367
Corbet R. H. D., 1986, MNRAS, 220, 1047
Fitzpatrick E. L., 1999, PASP, 111, 63
Halpern J. P., Tyagi S., 2005, The Astronomer's Telegram, 681
Horne K., 1986, PASP, 98, 609
Johnson H. L., Morgan W. W., 1954, ApJ, 119, 344
Kennea J. A., Racusin J. L., Burrows D. N., Hunsberger S., Nousek J. A., Gehrels N., 2005, The Astronomer's Telegram, 673
Landolt A. U., 1992, AJ, 104, 340
Lang K. R., 1999, Astrophysical Data: Planets and Stars. Springer-Verlag, New York
Leitherer C., 1988, ApJ, 326, 356
Makishima K., 1986, in Mason K. O., Watson M. G., White N. E., eds, Physics of Accretion on to Compact Objects. Springer, Berlin, p. 249
Masetti N. et al., 2006a, A&A, 449, 1139
Masetti N. et al., 2006b, A&A, 455, 11
Negueruela I., Schurch M. P. E., 2007, A&A, 461, 631
Negueruela I., Okazaki A. T., Fabregat J., Coe M. J., Munari U., Tomov T., 2001, A&A, 369, 117
Schmidt-Kaler Th., 1982, in Schaifers K., Voigt H. H., eds, Landolt-Bornstein Group VI, Vol. 2(b), Numerical Data and Functional Relationships in Science and Technology. Springer-Verlag, Berlin, p. 1
Steiner C., Eckert D., Mowlavi N., Decourchelle A., Vink J., 2005, The Astronomer's Telegram, 672
Stetson P. B., 1987, PASP, 99, 191
Stetson P. B., 1992, JRASC, 86, 71
Wegner W., 1994, MNRAS, 270, 229

This paper has been typeset from a TEX/LATEX file prepared by the author.